

MODEL GL0.2: AN IMPROVED CLEAR-SKY SOLAR IRRADIANCE ALGORITHM FOR LOWER AND UPPER ALTITUDE SITES

Part I: UV-VIS-NIR (UVNIR) MODEL

Juan C. Ceballos

Divisão de Satélites e Sensores Meteorológicos
Coordenação Geral de Ciências da Terra
Instituto Nacional de Pesquisas Espaciais

Abstract

It is presented an upgrade of GLo model (hereafter GL0.1) developed at 2000, which assess daily cycle of clear-sky solar irradiance and is included in CPTEC satellite-based GL models for solar irradiance. GL0.1 model considers solar irradiance as the sum of a component in UVVIS spectral interval (0.4-0.7 μm) subject to absorption/dispersion by the $\text{N}_2+\text{O}_2+\text{O}_3$ mixture, plus a component in solar IR interval (0.7-2.8 μm) with pure absorption by $\text{H}_2\text{O}+\text{CO}_2$. It must be noted that GL0.1 algorithm is suitable for sites at 1000 hPa level. Model GL0.2 has similar spectral partition enlarges surface pressure interval and improves associated algorithms.

This Part I describes improvements for UVVIS interval redefined as UVNIR λ :(0.2-0.8 μm). Detailed spectral analysis using STOCH2F stochastic model allows parameterization of integrated UVNIR irradiance for a given site, as a function of solar zenith angle and altitude.

Resumo

Apresenta-se um aperfeiçoamento do modelo GLo (no que segue, GL0.1) desenvolvido em 2000, o qual estima ciclo diurno de irradiância solar para céu claro está incluído nos modelos GL satelitais do CPTEC para irradiância solar. O modelo GL0.1 considera irradiância solar como a soma de uma componente UVVIS no intervalo espectral (0,4-0,7 μm) sujeita a absorção/dispersão numa mistura $\text{N}_2+\text{O}_2+\text{O}_3$, mais uma componente IR solar em (0,7-2,8 μm) com absorção pura por $\text{H}_2\text{O}+\text{CO}_2$. O algoritmo do GL0.1 é apropriado para locais no nível de 1000 hPa. O modelo GL0.2 tem partição espectral semelhante mas amplia o intervalo de pressões de superfície e aprimora os algoritmos associados.

Esta Parte I descreve os aprimoramentos para o intervalo UVVIS, redefinido como UVNIR λ :(0,2-0,8 μm). Uma análise espectral detalhada usando o modelo estocástico STOCH2F permite parametrizar a irradiância integrada em UVNIR para um dado local, como função do ângulo zenital solar e a altitude.

MODEL GL0.2: AN IMPROVED CLEAR-SKY SOLAR IRRADIANCE ALGORITHM FOR LOWER AND UPPER ALTITUDE SITES

Part I: UV-VIS-NIR (UVNIR) MODEL

June 2024

Content

Introduction

1. STOCHASTIC TWO-FLUX RADIATION TRANSFER SCHEME FOR UV-VIS-NIR INTERVAL

1.1. Foundations of stochastic two-flux (STOCH2F) radiative transfer model

1.2. Atmospheric profiles and optical parameters

1.3. Building stochastic model

1.4. Results

1.4.1. Fluxes for a black ground ($R_s = 0$)

1.4.2. Fluxes when $R_s > 0$: atmospheric counter-reflectance R^*

1.5. Conclusions

References

ANNEX 1. McClatchey atmospheres

ANNEX 2. Two-flux solutions for RTE

ANNEX 3. Radiative Code: Daily Cycle of UVNIR irradiance

Relatório de Pesquisa RT-GSTAR-002-2024

URL address - <http://pururuca.cptec.inpe.br/gstar/PUB/RTGSTAR/RTGSTAR0022024.pdf>

e-mail contact - gstar@inpe.br

INTRODUCTION

Clear-sky solar radiation models are useful because they provide reference values for assessing performance of radiometers, for basic estimations of radiative balance, and for models including the complex effect of gases, aerosol and cloud. A number of empirical and physical models have been published (Iqbal 1973, Barbaro et al. 1988, Antonanzas-Torres et al. 2019). In general, they present parameterizations which must be corrected in order to fit local characteristics. In this context, it is desirable to have a model requiring a set of few main physical variables and parameterizations as universal as possible.

Ceballos (2000) presented a simple physical model (hereafter called GL0.1) currently included in GL 1.2 solar radiation model (Ceballos et al. 2004) for clear-sky occurrence. It considers two spectral intervals exhibiting well defined phenomena: (a) ultraviolet-visible interval UVVIS:(0.3-0.7 μm), with ozone absorption and Rayleigh scattering; (b) solar infrared IRS:(0.7-2.8 μm), with pure absorption of direct beam by H_2O and CO_2 . Null aerosol load is assumed. If direct beam on the top of atmosphere (TOA) is S_0 with zenithal angle Z_0 ($\mu_0 = \cos Z_0$), $R_p(\mu_0)$ is planetary reflectance for a black ground ($R_s=0$) in UVVIS interval and ΔS the absorption of direct beam by water vapor and carbon dioxide, then irradiance G at ground level should be

$$G_{\text{UVVIS}}(\mu_0) = \mu_0 S_{0\text{UVVIS}} (1 - R_p - A); \quad (1)$$

$$G(\mu_0) = G_{\text{UVVIS}} / (1 - R_s R^*) + \mu_0 (S_{0\text{IRS}} - \Delta S). \quad (2)$$

In this model, $S_{0\text{UVVIS}}$ and $S_{0\text{IRS}}$ are partitions of solar constant. R_p for UVVIS interval is deducted from a whole-spectrum R_p algorithm of Lacis & Hansen (1974); it is assumed atmospheric absorptance $A=0$. ΔS depends on effective water vapor path $w_2 = w/\mu_0$ (w = precipitable water); parameterizations are deducted from Howard et al. (1956) and Roach (1961). GL0.1 algorithm is coherent with 1000 hPa pressure level; therefore, it

A three-part G-STAR document will present a revised version of GL0.1 model, labelled GL0.2. This report (Part I of the document) is concerned to 0.2-0.8 μm spectral interval. Main aspects:

- It still considers null aerosol load.
- Spectral intervals of GL0.2 are UVNIR:(0.2-0.8 μm), and IRS:(0.8-2.8 μm).
- Within UVNIR the stochastic two-flux code STOCH2F (Ceballos 2021) is used for detailed spectral description of radiative properties, including revision of counter-reflectance R^* and expected irradiance at altitudes z :(0-4 km), characteristic of mountainous areas in South America.
- G_{UVNIR} model includes planetary reflectance R_p and stratospheric absorption A .

Part II will criticize the water vapor absorption scheme used in GL0.1 and GL1.2 models and provide an updated algorithm which includes mean atmospheric pressure parameter, vertically weighted with precipitable water.

Part III will include UVNIR and IRS irradiances in GL0.2 model, with definition of geographic distribution of fundamental parameters over South America.

The model GL0.2 will be included in version GL 1.4 of GSTAR-INPE solar radiation model.

1. STOCHASTIC TWO-FLUX RADIATION TRANSFER SCHEME FOR UV-VIS-NIR (UVNIR) INTERVAL

Consider the atmosphere divided in N (horizontal) homogeneous layers, with direct beam S_0 (solar constant) impinging on the top of atmosphere (TOA) with zenith angle Z_0 ($\cos Z_0 = \mu_0$). Ground exhibits spectral reflectance $R_s(\lambda)$. For a site at altitude z , atmospheric depth in the geometric interval (z, ∞) corresponds to an optical depth τ for radiation with wavelength λ . Given monochromatic direct beam $S_{0\lambda}$ at TOA ⁽¹⁾, Beer's law describes its attenuation as

$$S_\lambda(\tau) = S_{0\lambda} \exp(-\tau/\mu_0). \quad (1.1)$$

Radiative transfer produces not only attenuation of direct beam, but also generates diffuse flux. Considering monochromatic radiative transfer (for the sake of simplicity: not using the subscript λ), the n -th layer located between optical depths $\tau=\tau_n$ and $\tau=\tau_n+\Delta_n$ will have *diffuse irradiances* E^\uparrow (ascendant) and E^\downarrow (descendant) described by

$$dE^\downarrow/d\tau' = -a_{11} E^\downarrow + a_{12} E^\uparrow + a_{13} S(\tau_n+\tau'), \quad (1.2.a)$$

$$dE^\uparrow/d\tau' = -a_{12} E^\downarrow + a_{22} E^\uparrow + a_{23} S(\tau_n+\tau'), \quad (1.2.b)$$

$$S(\tau_n+\tau') = S_0 \exp(-\tau'/\mu_0) = S(\tau_n) \exp(-\tau'/\mu_0). \quad (1.2.c)$$

Equations (1.2) are derived from the general Radiative Transfer Equation RTE (Liou 2002, Zdankowski et al. 2007) and constitute the two-flux model describing diffuse irradiances at optical depths $\tau' : [0, \Delta_n]$. Coefficients a_{ij} are in fact dependent on τ' , but can be assumed as a set of constant values within each layer, depending on simplifying hypotheses (Ceballos 1988, Meador and Weaver 1980, Liou 2002). The complete solution of eqs. (1.2) within N layers for $E_n^\downarrow, E_n^\uparrow$ must fulfill boundary conditions

$$E_1^\downarrow(0)=0 \quad (\text{first layer}) \quad (1.2.d)$$

$$E_n^\downarrow(\Delta_n) = E_{n+1}^\downarrow(0) \quad (\text{top of } n\text{-th layer, } n>1) \quad (1.2.e)$$

$$E_{n+1}^\uparrow(0) = E_n^\uparrow(\Delta_n) \quad (\text{base of } n\text{-th layer, } n<N) \quad (1.2.f)$$

$$E_N^\uparrow(\Delta_N) = R_s [\mu_0 S(\tau_N) + E_N^\downarrow(\Delta_N)]. \quad (\text{base of } N\text{-th layer}). \quad (1.2.g)$$

This procedure allows retrieval of irradiance profile but loses information about internal interactions among layers and radiative transfer. These interaction can be described by the stochastic scheme described in the next section.

1.1. Foundations of a stochastic two-flux (STOCH2F) radiative transfer model

Basic concepts of a stochastic two-flux model in N -layered atmospheres and some applications were developed in Ceballos (1986, 1989) and Souza et al. (19xx). Ceballos (2021)

¹ S_λ is a spectral density measured in units $W m^{-2} \mu m^{-1}$ *along the beam* (normal-incidence irradiance or directional flux), while direct irradiance or “direct radiation” is $E_\lambda = \mu_0 S_\lambda$.

presented a detailed description of STOCH2F code applied to radiative properties of clean atmospheres in 0.2-0.7 μm wavelength interval.

Considering irradiances $E_{\downarrow}(\tau')$, $E_{\uparrow}(\tau')$ referred to direct irradiance on the top of a layer, that is $\mu_0 S(\tau_n)$, they become variables $\zeta_{\downarrow}(\tau')$, $\zeta_{\uparrow}(\tau')$ and eqs. (1.2.a-c) can be written

$$d\zeta_{\downarrow}/d\tau' = -a_{11} \zeta_{\downarrow} + a_{12} \zeta_{\uparrow} + a_{13} \exp(-\tau'/\mu_0), \quad (1.3.a)$$

$$d\zeta_{\uparrow}/d\tau' = -a_{12} \zeta_{\downarrow} + a_{22} \zeta_{\uparrow} + a_{23} \exp(-\tau'/\mu_0). \quad (1.3.b)$$

For a single isolated layer, boundary conditions are $\zeta_{\downarrow}(0) = 0$, $\zeta_{\uparrow}(\Delta_n) = 0$. Their solutions yield transfer properties of the layer referred to incidence of direct radiation: T_o (diffuse transmittance), R_o (layer reflectance), A_o (layer absorptance):

$$\zeta_{\downarrow}(\Delta_n) = T_{o_n}, \quad \zeta_{\uparrow}(0) = R_{o_n}, \quad \exp(-\Delta_n/\mu_0) + T_{o_n} + R_{o_n} + A_{o_n} = 1. \quad (1.4)$$

Figure 1 illustrates how a beam of direct photons incident on the top of forth layer generates these four classes of flux.

For diffuse flux incident on top of a layer, $a_{13} = a_{23} = 0$ in eqs. (1.3). No direct beam is included; a single isolated layer requires the boundary conditions $\zeta_{\downarrow}(0) = 1$, $\zeta_{\uparrow}(\Delta_n) = 0$. Os fluxos through boundaries are diffuse transmittance T and reflectance R together with absorptance A , yielded by ⁽²⁾

$$\zeta_{\downarrow}(\Delta_n) = T_n, \quad \zeta_{\uparrow}(0) = R_n, \quad T_n + R_n + A_n = 1. \quad (1.5)$$

Consider the atmosphere as an N-layered system. Incidence of a beam of photons on top of atmosphere (TOA) leads to a set of “initial diffuse photon fractions”, with N descending diffuse fluxes at the bottom of layers, N ascending diffuse fluxes (at bottom of the layers also) and N absorbed fluxes (inside the N layers), plus a fraction escaping into sky from the first layer. This means a total of $3N+1$ “initial diffuse states” with two noteworthy observations: at the base of N-th layer there exist 1) null ascending flux, and 2) outgoing flux $E_{\text{exit}} = \mu_0 S_o \exp(-\tau/\mu_0)$ is a remaining direct irradiance.

Now let us include ground as a part of the whole system. Considering absorption within ground as “diffuse state”, then 1) a fraction R_s of E_{exit} is located as upward diffuse flux at N-th layer base, 2) a fraction $(1-R_s)$ is located at ground. In this way, direct irradiance at TOA is entirely transferred to $3N+2$ diffuse states. We can consider that two-flux radiative transfer exhibits a $(3N+2)$ -dimensional initial vector \mathbf{P}_o .

The initial diffuse photons start an up-and-down random walk until stopping in one of $N+2$ absorbing states. Single transfer process is realized jumping to neighboring layer; the physical properties reflectance, transmittance and absorptance (R_n , T_n , A_n) of the n-th visited layer can be assessed from eqs. (1.3) with the same boundary conditions but $a_{13} = a_{23} = 0$ (no direct radiation)⁽³⁾. Therefore, successive steps in random walk describe a sequence of vectors \mathbf{P}_o , \mathbf{P}_1 , \mathbf{P}_2 , ... following a first-order Markov process with transition probabilities described by basic properties (R , T , A).

In lieu of speaking about evolution of fractional numbers of photons, let's think about the process in terms of probability of states of a single photon. Solutions $\zeta_{n\downarrow}$, $\zeta_{n\uparrow}$ of equations (1.3) are *conditional probabilities* for a direct photon being located as a diffuse photon at the base (descending), at the top (ascending) and inside a layer, *given the incidence on the top of that*

² Provided that incident flux be isotropic, properties T , R , A are the same for incidence on the top (descendant flux) and on the bottom (ascendant flux).

³ Note that (R,T,A) are *not* (R_o,T_o,A_o) , and do not depend of incident angle Z_o .

layer. Probability of incidence at the top of that layer is $\exp(-\tau_{n-1}/\mu_0)$; thence initial probabilities composing $(3N+2)$ -dimensional vector \mathbf{P}_0 are

$$\text{Prob}\{\text{absorbed, sky}\} = R_0 \quad \{\text{state 1}\} \quad (1.5a)$$

$$\text{Prob}\{\downarrow, n\text{-th layer}\} = T_{0n} \exp(-\tau_{n-1}/\mu_0); \quad \{\text{states 21-38 in Figure 1}\} \quad (1.5b)$$

$$\text{Prob}\{\uparrow, n\text{-th layer}\} = R_{0n} \exp(-\tau_{n-1}/\mu_0); \quad \{\text{states 40-56}\} \quad (1.5c)$$

$$\text{Prob}\{\text{absorbed, } n\text{-th layer}\} = A_{0n} \exp(-\tau_{n-1}/\mu_0); \quad \{\text{states 3-20}\} \quad (1.5d)$$

$$\text{Prob}\{\uparrow, \text{ground}\} = R_s \exp(-\tau_N/\mu_0); \quad \{\text{state 39}\} \quad (1.5e)$$

$$\text{Prob}\{\text{absorbed, ground}\} = (1-R_s) \exp(-\tau_N/\mu_0); \quad \{\text{state 2}\} \quad (1.5f)$$

Figure 1 (right) illustrates the case of a 18-layer atmosphere, properly numbering the 56 diffuse states.

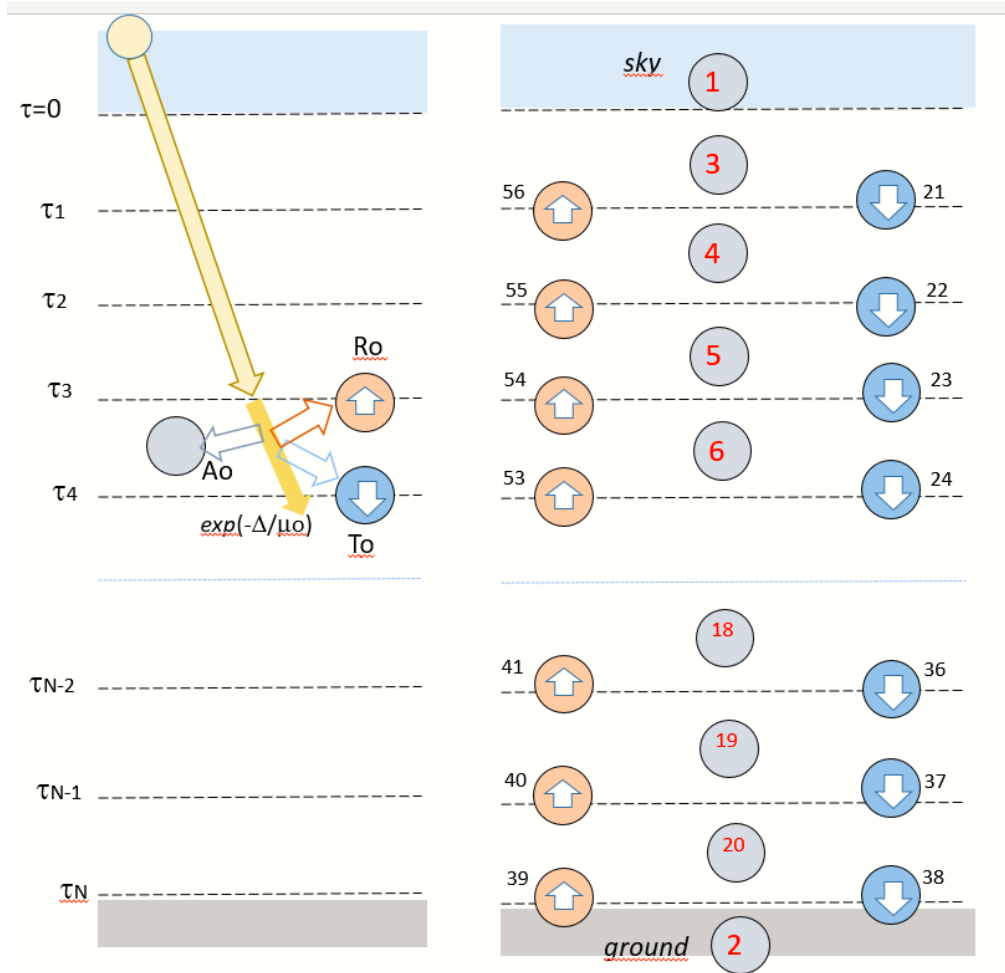


Figure 1. Two-flux radiative transfer. (left) Generation of initial diffuse photons. (right) States set for transitions a first-order Markov process, in an 18-layer atmosphere.

Figure 1 helps to describe the corresponding Markov transition matrix \mathbf{Q} (54×54). Diffuse photons transit to neighboring states such that, for instance, $Q(22,n) = 0$ except for $Q(22,5) = A_3$; $Q(22,23) = T_3$; $Q(22,55) = R_3$. Absorption states $n = 1-20$ have $Q(n,n) = 1$ that is, no further transitions are allowed. After infinite transitions photons are located at states 1-20 only.

Evolution $\mathbf{P}_0, \mathbf{P}_1, \dots, \mathbf{P}_{n \rightarrow \infty} = \boldsymbol{\pi}$ is described by

$$\mathbf{P}_n = \mathbf{P}_0 \mathbf{Q}^n, \quad \boldsymbol{\pi} = \mathbf{P}_0 \mathbf{Q}^\infty \quad (1.6)$$

Photons fate is unavoidable absorption at one of $N+2$ specific states, for which n -th components of vector $\boldsymbol{\pi}$ are not null. Choosing $n=1$ for “sky state” and $n=2$ for “ground state”, and given the spectral irradiance $\mu_0 S_\lambda$ at TOA within interval $\Delta\lambda$, then fundamental values for irradiances are

$$E_o = \int_{\Delta\lambda} \mu_0 S_\lambda d\lambda \rightarrow \text{incident irradiance at TOA} \quad (1.7)$$

$$E_r = \int_{\Delta\lambda} \pi_1(\lambda) \mu_0 S_\lambda d\lambda \rightarrow \text{reflected irradiance at TOA} \quad (1.8)$$

$$E_g = \int_{\Delta\lambda} \pi_2(\lambda) \mu_0 S_\lambda d\lambda \rightarrow \text{irradiance absorbed at ground} \quad (1.9)$$

$$G = \int_{\Delta\lambda} (1 - R_s)^{-1} \pi_2(\lambda) \mu_0 S_\lambda d\lambda \rightarrow \text{global radiation incident at surface} \quad (1.10)$$

Numbering with 3 to N the absorption states in layers 1 to N , if the base of N s-th layer is chosen as boundary between stratosphere and troposphere, then absorption probability and absorbed irradiance at stratosphere and troposphere are

$$\pi_{\text{strat}} = \sum_{n=3, N_s} \pi_n(\lambda) \rightarrow E_{\text{strat}} = \int_{\Delta\lambda} \pi_{\text{strat}}(\lambda) \mu_0 S_\lambda d\lambda, \quad (1.11)$$

$$\pi_{\text{trop}} = \sum_{n=N_s+1, N} \pi_n(\lambda) \rightarrow E_{\text{trop}} = \int_{\Delta\lambda} \pi_{\text{trop}}(\lambda) \mu_0 S_\lambda d\lambda. \quad (1.12)$$

Quotient between irradiances (1.8) to (1.12) and irradiance at TOA (1.7) yields corresponding fractional fluxes absorbed in those atmospheric regions.

1.2. Atmospheric profiles and optical parameters

Figure 2 illustrates profiles of air density and O_3 concentration for tropical (TROP) and mid-latitude winter (MLW) atmospheres, according to classical reference of McClatchey et al. (1972), divided in eighteen layers. Density profiles are similar, but O_3 profile shows differences, even when considering versions of McClatchey or Lacis and Hansen (1974), this last labelled “L&H”.

For two-flux radiative transfer within a layer the fundamental parameters are the triad (τ , ω , g): optical depth, single-scattering albedo and asymmetry factor, allowing definition of coefficients a_{ij} in Eqs. (1.3) in order to assess transfer properties of a given layer (see Annex 2).

Optical depth for a layer with geometrical thickness Δz is given by addition of Rayleigh (scattering) and O_3 (pure absorption) effects

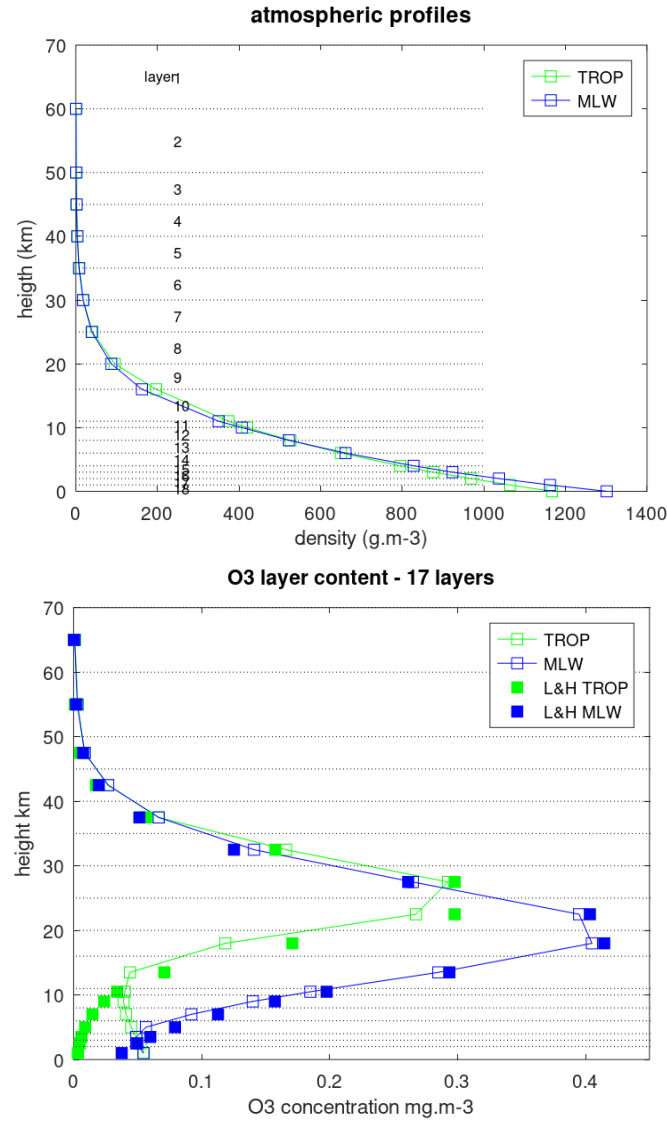


Figure 2. (*above*) Density profile for Tropical and Mid-latitude winter atmospheres at surface and at the top of 18 layers. (*below*) Similar for O3 density.

$$\tau = \tau_R + \tau_3, \quad (1.13a)$$

$$\tau_R = 0.00867 \lambda^{(-4.15+0.2 \lambda)} (\Delta P/P_o), \quad \lambda \text{ in } \mu\text{m}, \quad (1.13b)$$

$$\tau_3 = N_3 \sigma_3 \Delta z, \quad [N_3] = \text{molec m}^{-3}, \quad [\sigma_3] = \text{m}^2 / \text{molec}. \quad (1.13c)$$

Eq. (1.13b) improves usual algorithm for Rayleigh scattering optical depth (Paltridge e Platt 1976; Bodhaine et al. 1999); ΔP refers to pressure thickness of the layer, and $P_o = 1013 \text{ hPa}$. In Eq. (1.13c), N_3 can be deduced from McClatchey profiles (Annex 2) and molecular cross section σ_3 can be found in Ceballos (2021). Parameter ω describes probability of scattering in a single dispersion, estimated by

$$\omega = \tau_R / (\tau_R + \tau_3). \quad (1.14)$$

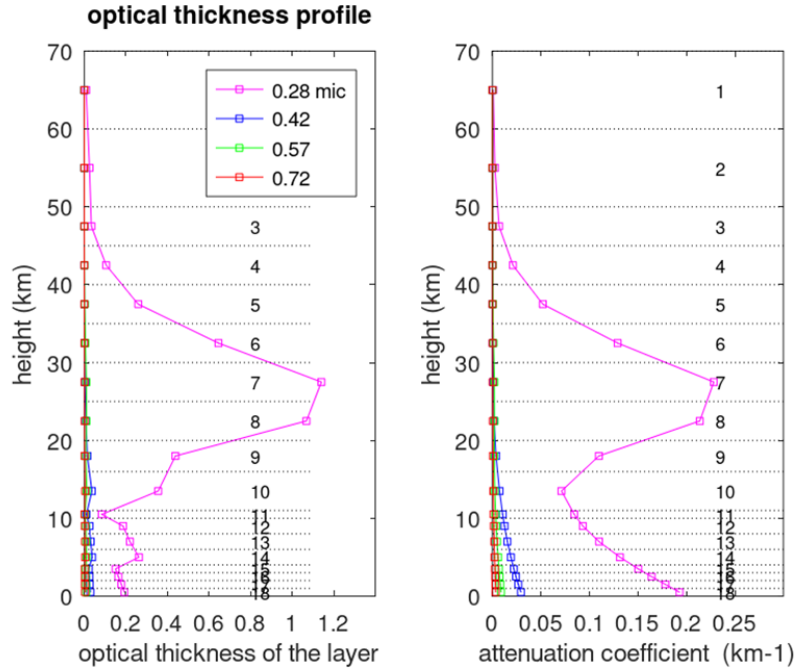


Figure 3. Optical depth of 18-layer TROP atmosphere, for 4 wavelengths, and attenuation coefficient for each layer.

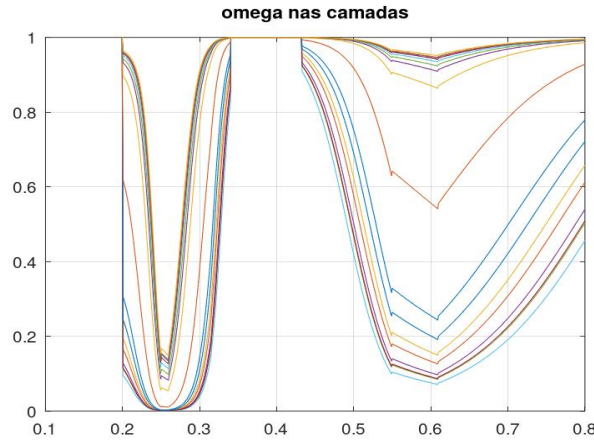


Figure 4. Spectrum of single-scattering coefficient within 0.2-0.8 μm interval for the 18 layers (1 to 18 from lower to higher ω values).

Figure 3 shows profile of τ and ω for the TROP McClatchey atmosphere. Optical depth seems to exhibit fluctuations at 6 and 14 km; actually, this is due to different geometric thicknesses δz ; when represented linear attenuation coefficient $k = \tau/\delta z$ we note the smooth variation of optical profile within the atmosphere. It must also be noted the influence of O_3 absorption for air+ O_3 mixture in the stratosphere, mainly in UV wavelengths as 0.28 μm , while air (O_2+N_2) Rayleigh scattering is predominant in the troposphere.

The ω spectrum in UV-VIS-NIR interval 0.2-0.8 μm shows the influence of the strong Hartley band in 0.20-0.315 μm , followed by the weaker Huggins band in 0.315-0.35 μm . Solar radiation with λ :(0.2-0.32 μm) must be strongly absorbed in every layer, *notably the incoming radiation* in the upper atmosphere. Above 0.36 μm radiative transfer is conservative except in

the Chappuis band interval (0.43-0.78 μm), which is weakly absorptive in the lower troposphere but can be proportionally very active in the stratosphere (although O_3 shows low optical depth, there is much lower conservative interaction with O_2+N_2 molecules).

Hereafter, we consider $z=16$ km as the limit between stratosphere and troposphere (base of ninth layer).

1.3. Building the stochastic model

McClatchey profiles were used in order to define 18 atmospheric layers (see Annex 1). Figures 2 illustrate pressure, air density and O_3 profiles. Each layer defines a triad $\{\tau \ \omega \ g\}$ where τ is optical depth, ω is single-scattering albedo and g is asymmetry factor. These ones are fundamental parameters for defining a_{ij} coefficients in Eqs. (1.3), as shown in Annex 2.

The scheme of stochastic states is illustrated by Figure 1. Solutions of Eqs. (1.3) for each layer (with upper and bottom blackbody boundaries) define direct transmittances and properties T_o , R_o , A_o (T_o , R_o being initial diffuse photon fluxes) allowing initial allocation of photons following Eqs. (1.5) for definition of initial vector P_o with dimension $N = 3 \times 18 + 2 = 56$. Absorbing states stay in sky (1), ground (2) and 18 layers (3-20). Solutions of Eqs. (1.3) with the same parameters a_{ij} but null direct incidence provide transition probabilities applied to k -th layer define properties T_k , R_k , A_k for diffuse photons; they fill the transition matrix $Q(N \times N)$. For instance, fourth layer has transition probabilities $Q(k1, k2) = Q(k1 \rightarrow k2)$

$$\begin{aligned} Q(23 \rightarrow 24) &= T_4, & Q(23 \rightarrow 54) &= R_4, & Q(23 \rightarrow 6) &= A_4, \\ Q(53 \rightarrow 54) &= T_4, & Q(53 \rightarrow 24) &= R_4, & Q(53 \rightarrow 6) &= A_4. \end{aligned}$$

Absorbing states $k1 = 1-20$ have $Q(k1 \rightarrow k1) = 1$. Other transitions have null probability.

The final vector was obtained for $n = 80$ iterations of transition process, that is

$$\pi = P_o Q^n, \quad n = 80. \quad (1.15)$$

The component π_2 describes ground absorption, while $G = \pi_2 / (1 - R_s)$ describes global irradiance, which includes the effects of first impact on ground (G_o) and of multiple reflections ground-atmosphere. The first is provided by π_2 if $R_s = 0$. For the second, a fundamental parameter is atmospheric counter-reflectance; this provided by π_2 considering $R_s = 0$ and components $P_o(k)$ of initial vector being $P_o(k=39) = 1$, $P_o(k \neq 39) = 0$, that is, first state emerging from ground.

Abovementioned procedure implies in having ground at $z=0$ (or $p_o = 1013$ hPa). If ground is located at a different altitude (say, the bottom of k_o -th layer, $k_o < 18$), properties of global irradiance are obtained in the same manner, except that layers $k > k_o$ must be eliminated. For instance, a scheme with atmospheric bottom at $z = 2$ km (see profile in Annex 1) implies in 16 layers with $p_o = 805$ hPa, $N = 3 \times 16 + 2 = 50$ states, absorbing states 1-18, downward states 19-34, upwelling states 35-50. Radiative properties of each layer are the same abovementioned for layers 1-16. Clearly, $Q(34,2) = 1 - R_s$, $Q(34,35) = R_s$.

1.4. Results

Fluxes for black ground ($R_s = 0$).

Figure 5 illustrates spectral probabilities and irradiances for black ground and surface pressure $p_0 = 1013$ hPa. The first observation is that UV absorption virtually reduces UV solar constant from 111 to effective 95 Wm^{-2} in $\lambda: (0.3-0.4 \mu\text{m})$, and UVNIR from 772 Wm^{-2} in $\lambda < 0.8 \mu\text{m}$ interval to 757 Wm^{-2} over an effective interval $\lambda: (0.3-0.8 \mu\text{m})$ (solar spectrum following Gueymard 2004).

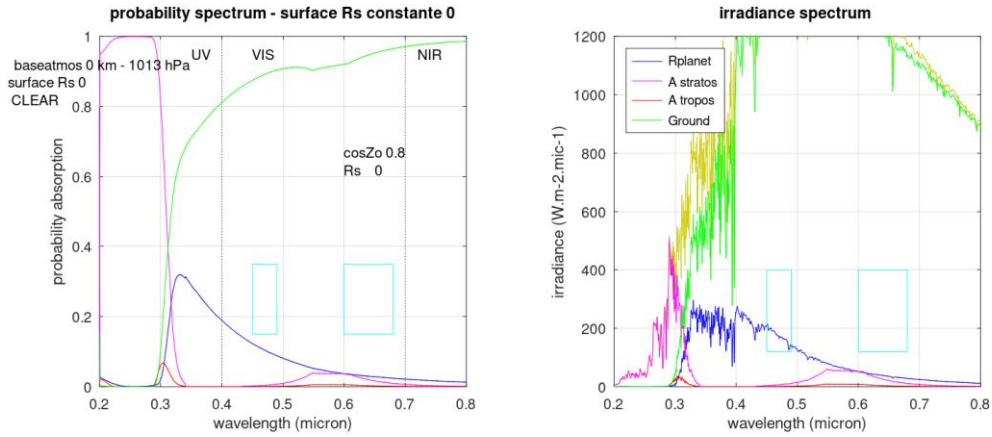


Figure 5. (left) Spectrum of absorption probabilities (at sky, within stratosphere, within troposphere and at ground, ground reflectance being $R_s=0$). (right) Corresponding spectral irradiances.

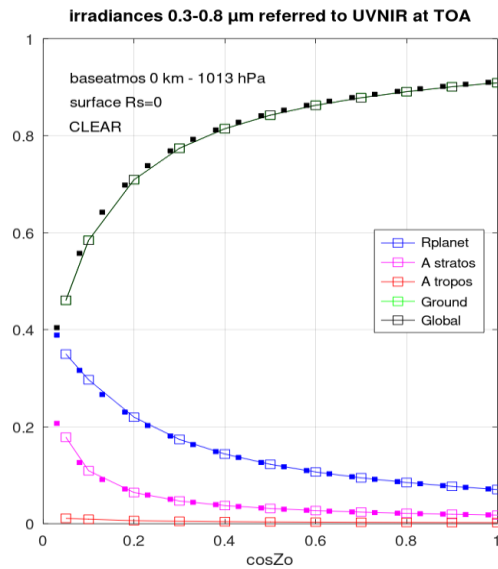


Figure 6. Dependence of (integrated) relative UVNIR irradiances and absorptions on solar zenith angle. Tropical atmosphere, ground level ($p_0 = 1013$ hPa) with black ground.

Figure 6 shows the results for a tropical atmosphere with pressure 1013 hPa at $z=0$, integrated over $\lambda:(0.3-0.8 \mu\text{m})$. Given that absorption within troposphere is negligible, energy balance in UVNIR interval becomes

$$\mu_0 S_{\text{UVNIR}} \approx (R_p + A_s) \mu_0 S_{\text{UVNIR}} + G_{\text{UVNIR}}. \quad (1.15)$$

R_p and A_s are planetary reflectance and stratospheric absorptance, referred to UVNIR irradiance on TOA. Defining atmospheric (global) transmittance as K_{to} , we have

$$K_{\text{to}} = G_{\text{UVNIR}} / \mu_0 S_{\text{UVNIR}} = 1 - R_p - A_s. \quad (1.16)$$

Figure 6 includes numerical results of STOCH2F (empty squares), as well as the interpolations of R_p and A_s (filled squares) found by fitting functions

$$y = (a + b \mu_0 + c \mu_0^2)^{-1}. \quad (1.17)$$

This expression seems excellent for model parametrizations.

R_p , A_s , G_o values for various atmospheric columns is obtained by successive elimination of lowest pressure level in profile data (see Annex 1), up to $z=6$ km altitude. Resultant bases of atmosphere (with 18 to 13 layers) follow the Table below.

Yz= [...							
%	z	dens	po	O3	dens	po	O3
	06	650	492	4.30	661	463	6.4; ...
	04	795	633	4.70	828	608	4.9; ...
	03	876	715	5.10	923	694	4.9; ...
	02	969	805	5.40	1037	790	4.9; ...
	01	1064	904	5.60	1162	897	5.4; ...
	00	1167	1013	5.60	1301	1018	6.0];

STOCH2F applied to these atmospheres yields the sequence of coefficients (a_r , b_r , c_r) for reflectance and (a_a , b_a , c_a) for absorptance, as follows.

abcRA= [...									
%	n	z	po	a_r	b_r	c_r	a_a	b_a	c_a
	0	0	1013	2.2186	11.777	.1778	2.953	62.92	-10.32; ...
	1	1	904	2.2580	13.222	.1679	2.939	63.28	-9.97; ...
	2	2	805	2.2987	14.874	.1550	2.926	63.63	-9.62; ...
	3	3	715	2.3409	16.775	.1368	2.912	63.97	-9.27; ...
	4	4	633	2.4324	19.345	.0911	2.899	64.31	-8.92; ...
	5	6	492	2.4762	24.484	.0706	2.869	65.02	-8.32];

In the first column, n means the number of levels eliminated and (z , po) the altitude and pressure of the new base of atmosphere. Eq. (1.17) can be expressed as

$$R_p = A_r / (1 + B_r \mu_0 + C_r \mu_0^2); \quad (1.18a)$$

$$A_s = A_a / (1 + B_a \mu_0 + C_a \mu_0^2). \quad (1.18b)$$

We can expected that coefficients (A , B , C) vary with total pressure (that is, with the amount of optical path in the column); Figure 7 illustrates dependence on po .

Concerning R_{p0} , 1) A_r can be considered nearly constant within 5%; 2) B_r is the main factor in Eq. (1.18a) and clearly depends on pressure po ; 3) C_r is also variable with po , but as a weaker

contribution to R_p . In order to assess A_{so} in stratosphere (eq. 1.18b), (A_a , B_a , C_a) can be considered constant within 1-2%. Interpolated coefficients (pressure p_0 in hPa) are:

$$P = p_0/1000; [p_0] = \text{hPa};$$

$$A_r = 0.353 + 0.099 P, \quad \text{or} \quad 0.43 \pm 0.02; \quad (1.19a)$$

$$B_r = \beta P^\alpha, \quad \beta = 5.369, \quad \alpha = -0.860;$$

$$C_r = 1.309 P^3 - 3.530 P^2 + 3.216 P - 0.915;$$

$$A_a = 0.342 \pm 0.003; \quad (1.19b)$$

$$B_a = 21.7 \pm 0.4,$$

$$C_a = -3.28 \pm 0.20.$$

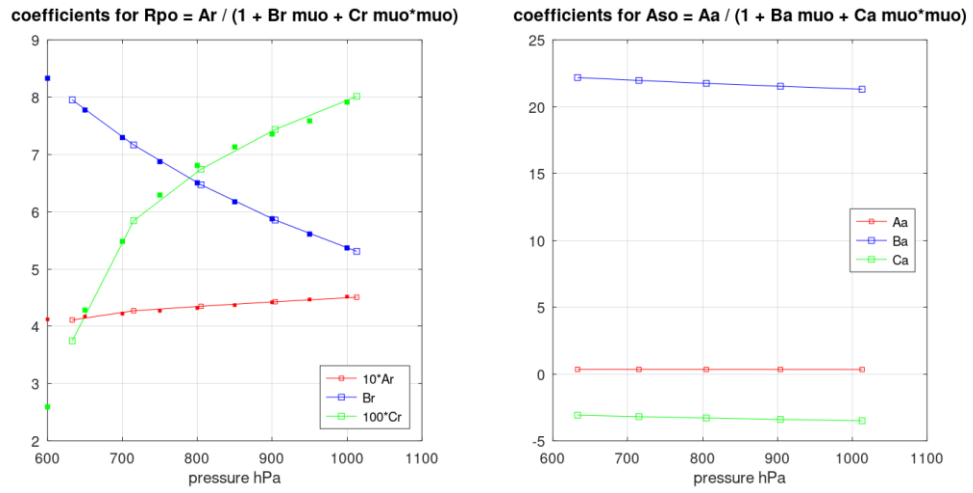


Figure 7. Variability of coefficients (A, B, C) with total pressure at ground level. Empty squares indicate values obtained by STOCH2F. Filled squares illustrate interpolations (Eqs. 1.19).

Atmospheric counter-reflectance R^*

Atmospheric base levels $z_{base} = 0, 1, 2, 3, 4$ km were considered, thus the number of layers was $N = 18, 17, 16, 15, 14$. Initial state was $2N+3$ (z_{base} , ascending). Black ground ($R_s=0$) implies in escape to sky (transmittance T^*) and return probability (counter reflectance R^*) given by π_1 and π_2 components. Absorption in the atmosphere is assessed by $A^* = 1 - \pi_1 - \pi_2$. Figures 8 show the spectral results for z_{base} at 0 km and 4 km. Following Figures 5 and 8 we can assume an effective spectral lower limit $\lambda_o = 0.3 \mu\text{m}$; below this limit, not only O₃ absorption is high but irradiance arriving to ground is negligible.

It is noteworthy that $R_{troplayer} = R^*$ estimated for a Rayleigh atmosphere in a troposphere with top level at 50 hPa (Eq. A2.7b) closely follows estimates of STOCH2F for $\lambda > \lambda_o$. This should be expected, since upward diffuse photons going into stratosphere exhibit a very low probability of return to the surface (Figure 8 includes the curve $R^*_{stratos} = \pi_2$ obtained for initial state upward at the base of stratosphere, be 39 if $N = 18$, $z_{base}=0$, or 31 if $N=14$, $z_{base}=4$ km).

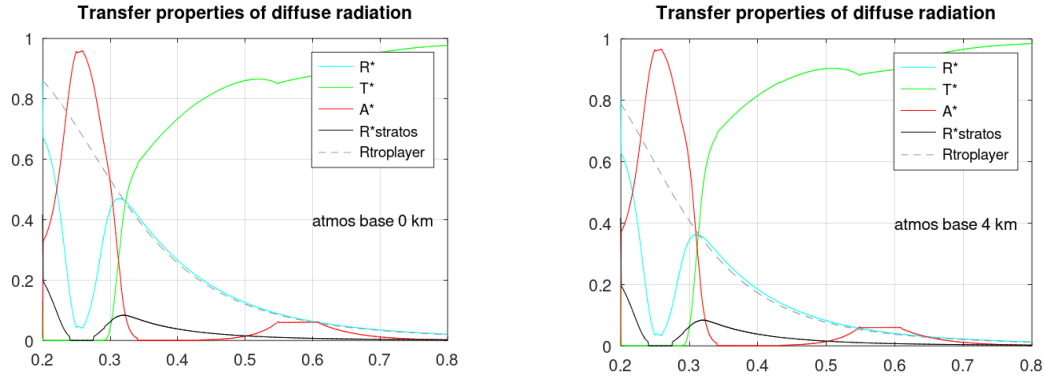


Figure 8. Transmittance T^* , Counter-reflectance R^* and absorption A^* for a diffuse photon starting upward at ground level. Two TROP atmospheres extend through $z:(z_{\text{base}} - \infty)$, with $z_{\text{base}} = 0$ and $z_{\text{base}} = 4$ km. Also included: (a) probability of return to ground, starting upward at the base of stratosphere (black line); (b) counter-reflectance R_o^* for a Rayleigh atmosphere with the top at 50 hPa be $z:(z_{\text{base}} - \text{about } 20 \text{ km})$, dashed gray line.

Given absorption $G_o = \pi_2(R_s = 0)$ in a black ground, no counter-reflection happens; thence for $R_s > 0$ we can assume G_o as a first contribution to surface irradiance followed by multiple atmospheric reflections. The monochromatic version of an UVNIR model for global radiation becomes

$$G = G_o + G_o \cdot R_s R^* + (G_o R_s R^*) \cdot R_s R^* + \dots = G_o / (1 - R_s R^*). \quad (1.20)$$

This is equivalent to STOCH2F estimate $\pi_2(R_s > 0)/(1 - R_s)$. G_o is a function of (λ, μ_o) , R^* being only of λ . We can define a mean value R^{**} over UVNIR interval $\lambda:(0.3-0.8 \mu\text{m})$; in terms of irradiances K_{to} , K_t ,

$$E_{oo}(\mu_o) = \int_{\text{UVNIR}} \mu_o S_{o\lambda} d\lambda, \quad (1.21a)$$

$$E_o(\mu_o) = \int_{\text{UVNIR}} G_o(\lambda; \mu_o) \mu_o S_{o\lambda} d\lambda = K_{to} E_{oo}, \quad (1.21b)$$

$$E(\mu_o) = \int_{\text{UVNIR}} G_o(\lambda; \mu_o) (1 - R_s R^*)^{-1} \mu_o S_{o\lambda} d\lambda = K_t E_{oo}, \quad (1.21c)$$

$$K_t = K_{to} / (1 - R_s R^{**}). \quad (1.21d)$$

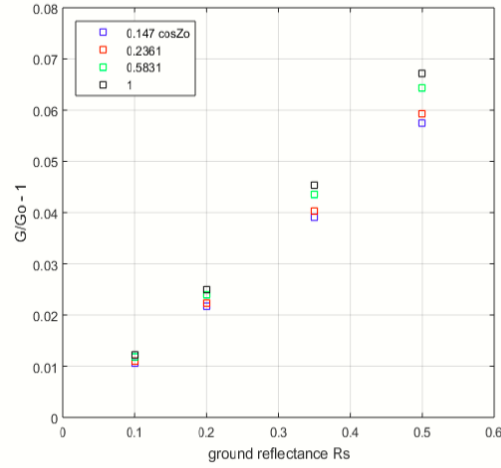


Figure 9. Evidence of linearity of $(E/E_o - 1)$ versus R_s for different values of Z_o (Source: Ceballos 2021)

Considering a TROP McClatchey atmosphere, surface pressure 1013 HPa, Ceballos (2021) found evidence of nearly constant values of R^{**} . Figure 9 presents data of $(K_t/K_{t0} - 1)$ versus R_s for several values of μ_o and R_s for interval λ : (0.2-0.8 μm). It is evident a linearity of the whole set yielding constant values R^{**} independent of R_s but shows some variability with Z_o ($R^{**} \approx 0.119$ for $Z_o > 76^\circ$ and $R^{**} \approx 0.134$ for $Z_o < 60^\circ$). In order to inspect variability of R^{**} with altitude and solar zenith angle, we considered $R_s = 0.3$ and λ : (0.3-0.8 μm) as effective interval. Figure 3 resumes results of using spectral probabilities G_o , G and Eqs. (1.21) allowed to build Figure 10.

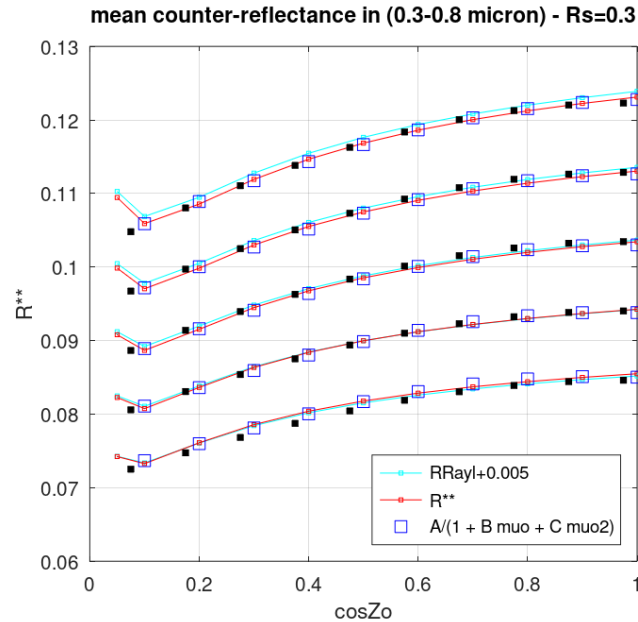


Figure 10. Mean counter-reflectance over UVNIR, following (a) $R^*(\lambda)$ estimate following Rayleigh scattering; (b) $R^*(\lambda)$ estimate from STOCH2F; (c) interpolation of case (b). Black squares show result of a general interpolation (see text).

- Mean counter-reflectance varies slowly with $\mu_0 = \cos Z_0$, and with altitude z (km), between 0.073 and 0.123. Curves in Figure 10 correspond to the sequence $z = 0, 1, 2, 3, 4$ km for the base of troposphere. Irregular behavior for $\mu_0 < 0.1$ ($Z_0 > 84^\circ$) is due to shortcomings of STOCH2F algorithm for near horizontal solar beam.
- Rayleigh-based and STOCH2F values R^* yield nearly the same mean value: $R^{**}(\text{STOCHF}) = R^{**}(\text{Rayleigh2F}) + 0.005$;
- R^{**} can be accurately described by an algorithm $R^{**}(\mu_0, z) = A / (1 + B \mu_0 + C \mu_0^2)$, where A, B, C are functions of altitude. Nevertheless, B and C are much less variable than A , replaced by their mean value in $z: (0-4 \text{ km})$.

An accurate final algorithm for TROP atmosphere (black squares in Figure 10) is

$$R^{**}(\mu_0, z) = A(z) / (1 + B_{\text{med}} \mu_0 + C_{\text{med}} \mu_0^2), \quad (1.22)$$

$$A = 0.102 - 0.008 z(\text{km}), \quad B_{\text{med}} = -0.334 \pm 0.020, \quad C_{\text{med}} = 0.171 \pm 0.015.$$

Application: a daily cycle for GLuvnir

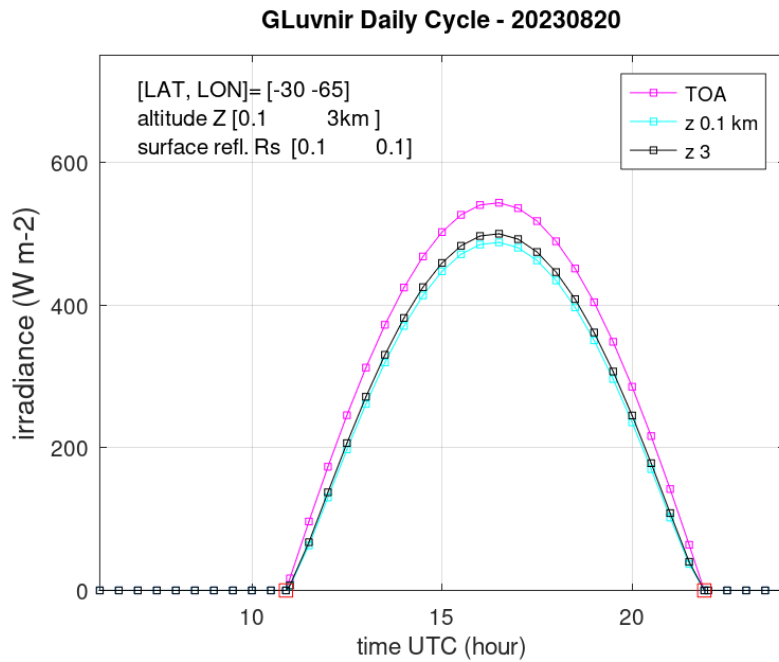


Figure 11. Daily cycle of GLuvnir for 20230820 at a site located at -30° latitude, -65° longitude, for two altitudes: 100 m and 3000 m. MLW atmospheric profile was assumed.

The set of resultant parameterizations was applied to estimate $K_t(\mu_0)$ (eq. 1.21d) and corresponding irradiance $GLuvnir = \mu_0 \cdot S \cdot K_t$ at altitude $z = 100\text{m}$ and 3000m . Figure 11 illustrates results.

1.5 CONCLUSIONS

Ozone absorption+Rayleigh attenuation in UV, together with weak spectral irradiance at TOA, strongly reduce surface global irradiance G_o in $\lambda < 0.3 \mu\text{m}$; therefore, $\Delta\lambda: (0.3-0.8 \mu\text{m})$ should be assumed as effective UVVISNIR (here called UVNIR) interval. Tropospheric pressure profile $p(z)$ is not actually important, because optical depth τ (and scattering processes) depends only on pressure value, that is, total optical path. Therefore, Tropical (TROP) McClatchey profile was considered.

Clear-sky irradiance GL in UVNIR: $(0.3-0.8 \mu\text{m})$ for a clean atmosphere (without aerosol) can be described by simple algorithms. For solar zenith angle Z_o ($\mu_o = \cos Z_o$) with black surface ($R_s = 0$) and altitude z km (corresponding pressure p_o hPa),

$$GL_o(\mu_o) = \mu_o S_{UVNIR} (1 - R_{po} - A_{so}),$$

$$R_{po} = A_r / (1 + B_r \mu_o + C_r \mu_o^2),$$

$$A_{so} = A_a / (1 + B_a \mu_o + C_a \mu_o^2),$$

- $S_{UVNIR} = 757 \text{ W m}^{-2}$: directional solar flux in UVNIR interval, mean Earth-Sun distance
- $\mu_o = \cos Z_o$, Z_o solar Zenith angle
- $R_{po}(\mu_o, p_o)$: local planetary reflectance related to TOA irradiance in $\Delta\lambda$
- $A_{so}(\mu_o, p_o)$: local stratospheric absorption related to TOA irradiance in $\Delta\lambda$
- $A_r, B_r, C_r, A_a, B_a, C_a$: coefficients depending on pressure at atmospheric base. Described by Eqs. (1.19).

For actual surfaces ($R_s > 0$ typical value in $\Delta\lambda$), multiple reflections surface-troposphere increase original irradiance GL_o through a simple algorithm

$$GL(\mu_o, R_s) = GL_o(\mu_o) / (1 - R_s R^{**}),$$

$$R^{**} = A(z) / (1 + B_{med} \mu_o + C_{med} \mu_o^2),$$

- R_s = ground reflectance in UVNIR interval
- $R^{**} =$ mean value of atmospheric counter-reflectance in UVNIR, Eqs. (1.22). It is essentially not dependent on R_s but on altitude z , and weakly on μ_o .
- R^{**} is counter-reflectance $R^*(\lambda)$ weighted with spectral $GL_o(\lambda)$ obtained by STOCH2F. It is noteworthy the fact that R^* obtained through STOCH2F as well as a simple algorithm based on 2-flux equations applied to a ($p_o - 50$ hPa) atmospheric layer allow spectral integration of $GL_o / (1 - R_s R^*)$ with the same quality of results.

When applying GL 0.2 parameterizations to sites of different altitudes, it is seen that a clean clear-sky atmosphere has significant influence on UVNIR irradiance. For the chosen day and local, it is about 55 Wm^{-2} ; however, the difference between two altitude cases ($z = 100\text{m}$ and $z = 3000\text{m}$) does not exceed 12 Wm^{-2} . The results suggest that clean atmosphere has a typical influence on surface irradiance, with lower impact of altitudes between 0 and 4000m. Higher impact of altitude could be expected concerning aerosol concentrated within planetary boundary layer ($z < 2000\text{m}$), and/or absorption by H_2O vapor in IRS interval. Precipitable water shows a

steeper decrease with altitude. This last influence is the subject of Part II of this research for GL 0.2 model.

Routines (Octave compatible) are included in Annex, for estimation of GL_{UVNIR} as a function of date and hour, and local latitude/longitude/altitude.

REFERENCES

- Antonanzas-Torres, F., R. Urraca, J. Polo, O. Perpiñán-Lamigueiro, R. Escobar (2019). Clear sky solar irradiance models: A review of seventy models. *Renewable and Sustainable Energy Reviews* 107:374-387. <https://doi.org/10.1016/j.rser.2019.02.032>
- Barbaro, S., G. Cannistraro, C. Giaconia, A. Orioli (1988). The ASHRAE clear sky model. An evaluation in the Mediterranean Zone. *Solar and Wind Technology* 5: 111-116.
- Bodhaine, B.A., N.B. Wood, E.G. Dutton, J.R. Slusser (1999). On Rayleigh optical depth calculations. *J. Atmos. Ocean. Technol.* v. 16:1854-1861.
- Ceballos, J.C. (1986). *Um modelo estocástico de propagação da radiação solar na atmosfera* (A stochastic model for solar radiative transfer in the atmosphere). PhD Thesis, Instituto Astronômico e Geofísico, Universidade de São Paulo. 376 pp.
- Ceballos, J.C. (1988). On two-flux approximations for shortwave radiative transfer in the atmosphere. *Contributions to Atmospheric Physics*, v. 61:10-22.
- Ceballos, J.C. (1989). Stochastic properties of two-flux shortwave radiative transfer in the atmosphere. *Contributions to Atmospheric Physics* v. 62:180-192.
- Ceballos, J.C. (2000). Estimativa de radiação solar à superfície com céu claro: Um modelo simplificado. *Revista Brasil. de Meteorologia* 15: 113-122.
- Ceballos, J.C. (2021). *STOCH2F: Stochastic two-flux code for diagnosis and assessment of solar radiative fluxes in the atmosphere. Part 1: 0.20-0.80 μm interval in clean clear-sky atmosphere.* Research Report RT-GSTAR-001-2021. [LNK](#)
- Gueymard, C.A. (2004). The sun's total and spectral irradiance for solar energy applications and solar radiation models. *Solar Energy* v. 76(4):423-453 (doi: 10.1016/j.solener.2003.08.039) Howard Burch Williams 1956
- Iqbal, M. (1983). *An introduction to solar radiation*. Academic Press, 390 pp.
- Lacis, A.A., J.E. Hansen (1974). A parameterization for the absorption of solar radiation in the Earth's atmosphere. *J. Atmos. Sci.* v.31, 118-133.
- Lefèvre, M., A. Oumle, P. Blanc, B. Espinar et al. (2013). McClear: a new model estimating downwelling solar radiation at ground level in clear-sky conditions. *Atmos. Meas. Tech.* v.6, 2403-2418. doi:10.5194/amt-6-2403-2013.
- Liou, K.N. (2002). *An introduction to atmospheric radiation*. Academic Press, 2nd Ed., 577 pp.
- López, G., F.J. Batlles, J. Tovar-Pescador (2007). A new simple parameterization of daily clear-sky global solar radiation including horizon effects. *Energy Conversion and Management* 48:226-233. doi:10.1016/j.enconman.2006.04.019
- McClatchey, R.A., R.W. Fenn, J.E.A. Selby, F.E. Volz, J.S. Garing (1972). *Optical properties of the atmosphere*, Third Ed. Air Force Cambridge Research Laboratories, Environ. Res. Papers No 411.
- Meador, W.E., W.R. Weaver (1980). Two-stream approximations to radiative transfer in planetary atmospheres: A unified description of existing methods and a new improvement. *J. Atmos. Sci.* v. 37:630-643.
- Paltridge, G.W., C.M.R. Platt (1976). *Radiative processes in Meteorology and Climatology*. Elsevier Sci. Pub. Co.

- Roach, W.T. (1961). The absorption of solar radiation by water vapour and carbon dioxide in a cloudless atmosphere. *Quarterly J. of the Meteor. Soc.* 87:354-373.
- Salazar, G., A.L. Hernández, L.R. Saravia (2010). Practical models to estimate horizontal irradiance in clear sky conditions: Preliminary results. *Renewable Energy* 35:2452-2460. doi:10.1016/j.renene.2010.01.033
- Souza, J.D., B.B. Silva, J.C. Ceballos (2008). Estimativa de radiação solar global à superfície usando um modelo estocástico: Caso sem nuvens (Estimate of global solar radiation at ground level using a stochastic model: Cloudless case). *Rev. Brasil. de Geofísica*, v. 26(1):31-44.
- Zdunkowski, W., Th. Trautmann, A. Bott 2007. *Radiation in the Atmosphere. A Course in Theoretical Meteorology*. Cambridge Un. Press. Paperback Edition 2018.

ANNEX 1: McClatchey profiles

TROP: Tropical, MLW: MidLatitude Winter

% ----- 18 layers original McClatchey ---									
%	z	---	TROP	-----		---	MLW	-----	
%	z	ro	p	O3	U	ro	p	O3	U
Yz= [...									
	70	.09	.058	.008	1.4e-7	0.07	.047	.01	1.4e-7; ...
	60	.60	.40	.21	...	0.48	.300	.15	... ; ...
	50	1.1	.85	.43	6.3e-6	0.89	.682	.43	6.3e-6; ...
	45	2.1	1.59	1.3	1.9e-5	1.74	1.29	1.3	1.9e-5; ...
	40	4.2	3.0	04.1	4.3e-5	3.62	2.53	4.1	4.3e-5; ...
	35	08.6	6.0	09.2	1.1e-4	7.92	5.18	9.2	1.1e-4; ...
	30	18.3	12.2	24.0	3.6e-4	17.8	11.1	19.0	3.6e-4; ...
	25	40.4	25.7	34.5	6.7e-4	39	24.3	34.0	6.7e-4; ...
	20	95.1	56.5	19.0	4.5e-4	87	53.7	45.0	4.5e-4; ...
	16	197	111	4.7	6.4e-4	162	101	36.0	6.4e-4; ...%stra
	11	374	247	4.1	0.017	350	220	21.0	6.9e-3; ...
	10	420	286	3.90	0.05	407	257	16.0	7.5e-3; ... %Ci
	08	526	378	3.90	0.25	522	347	12.0	0.035; ...
	06	650	492	4.30	0.85	661	463	6.4	0.21; ...
	04	795	633	4.70	2.2	828	608	4.9	0.66; ...
	03	876	715	5.10	4.7	923	694	4.9	1.2; ... %ST
	02	969	805	5.40	9.3	1037	790	4.9	1.8; ...
	01	1064	904	5.60	13.0	1162	897	5.4	2.5; ...
	00	1167	1013	5.60	19.0	1301	1018	6.0	3.5];

Physical variables are defined for a level z (first column). Layer values are calculated as arithmetic mean between top and bottom of the layer.

Units:

z(km), ro: density(g m⁻³), p(hPa), O3(g m⁻³), U: humidity(g m⁻³)

Relationship z(altitude km) → p(pressure level hPa): interpolation of Table data for z<=8 km yields

$$p(z=0)/p(z) = 1.0112 + 0.0885 z + 0.0149 z^2 \quad (\text{TROP}), \quad (\text{A1.1})$$

$$p(z=0)/p(z) = 1.0158 + 0.0927 z + 0.0182 z^2 \quad (\text{MLW}). \quad (\text{A1.2})$$

Deviation from the quotient is about +0.01 for z=0, being generally lower for higher levels. A simple exponentially decreasing fit for pressure shows higher deviations.

Parameterization of relationship p(pressure level hPa) → z(altitude km) :

$\eta = p/p_0$, with $p_0 = 1000$ hPa, yields

$$z = 15.574 - 23.063 \eta + 7.632 \eta^2 \quad (\text{TROP}), \quad (\text{A1.3})$$

$$z = 14.757 - 22.330 \eta + 7.7401 \eta^2 \quad (\text{MLW}) \quad (\text{A1.4})$$

Deviations are lower than 50 m if z<6 km.

ANNEX 2. Two-flux solutions for RTE

In order to describe upward E^\uparrow and downward E^\downarrow diffuse irradiances, the general RTE is reduced to a pair of first-order differential equations (τ' = optical depth; $\mu_0 = \cos Z_0$; τ = total optical depth)

$$d\zeta^\downarrow/d\tau' = -a_{11} \zeta^\downarrow + a_{12} \zeta^\uparrow + a_{13} \exp(-\tau'/\mu_0), \quad (A2.1.a)$$

$$d\zeta^\uparrow/d\tau' = -a_{12} \zeta^\downarrow + a_{22} \zeta^\uparrow + a_{23} \exp(-\tau'/\mu_0), \quad (A2.1.b)$$

where irradiances are related to that incident on layer top: $\zeta^\uparrow\downarrow = E^\uparrow\downarrow(\tau')/E^\downarrow(0)$. Coefficients are

$$a_{11} = [1 - \omega(1 - \langle b^\downarrow \rangle)] / \langle \mu^\downarrow \rangle - Edd \quad a_{12} = \omega \langle b^\uparrow \rangle / \langle \mu^\uparrow \rangle - Edd \quad (A2.2.a)$$

$$a_{21} = \omega \langle b^\downarrow \rangle / \langle \mu^\downarrow \rangle - Edd \quad a_{22} = [1 - \omega(1 - \langle b^\uparrow \rangle)] / \langle \mu^\uparrow \rangle - Edd \quad (A2.2.b)$$

$$a_{13} = \omega(1 - b_0) \quad a_{23} = -\omega b_0 \quad (A2.2.c)$$

Exponential function in Eqs. (A2.1) describes attenuation of direct beam. Parameter b_0 is backscattered fraction for incident beam with zenithal angle Z_0 and describes probability of conversion to upward diffuse irradiance for scattered radiation. If only diffuse radiation propagates, then $a_{13} = a_{23} = 0$.

$Edd=0$ and $g=0$ if pure isotropic radiation is assumed (Schuster-Schwartzschild approximation). Eddington (EDD) approximation admits axial symmetry around vertical direction (radiance is a function of τ' and μ_0) so that $g>0$ and $Edd=1/4$.

Brackets $\langle X \rangle$ refer to *hemispherical* mean value of a variable $X(\tau', \Omega)$ which is a function of all directions Ω . It is the case of diffuse radiance L , $\cos Z$ and backscattered fraction $b(\Omega^i)$, Ω^i = incident direction (Ceballos 1986 and 1988, Zdunkowski et al. 2007). For downward diffuse radiance,

$$\langle X^\downarrow \rangle = \int_{+2\pi} X(\Omega) L(\Omega) d\Omega / \int_{+2\pi} L(\Omega) d\Omega \quad (A2.3)$$

If diffuse radiance can be considered hemispherically isotropic, that is $L(\tau', \Omega^\downarrow) = L^+(\tau')$ and $L(\tau', \Omega^\uparrow) = L^-(\tau')$, then ⁽⁴⁾

$$\langle \mu^\downarrow \rangle = \langle \mu^\uparrow \rangle = \mu_m = 1/2, \quad \langle b^\downarrow \rangle = \langle b^\uparrow \rangle = b_m, \quad \alpha = b_m / \mu_m. \quad (A2.4)$$

Parameters b_0 , b_m are defined by the scattering phase function $P(\Omega', \Omega)$, with Ω' being incident direction and Ω scattered direction ⁽⁵⁾, with first-order approximations

$$b_0(\mu_0) = (1/4\pi) \int_{2\pi} P(\Omega_0, \Omega) d\Omega \approx 1/2(1 - 3g\mu_0/2), \quad (A2.5)$$

$$b_m \approx 1/2(1 - 3g/4). \quad (A2.6)$$

Integration is performed over backscattering hemisphere; eq. A2.6 assumes incidence of isotropic incident radiance.

Assuming hemispherical isotropy for diffuse radiance,

⁴ EDD approximation operates considering hemispherical isotropy and the correction $Edd=1/4$. It could be suitable even for nearly isotropic Rayleigh scattering, in case of strong absorption (for instance, for UV radiation in Hartley-Huggins band interval).

⁵ Phase function is a probability density, so that $(1/4\pi) P(\Omega', \Omega) d\Omega$ is the probability of a photon with incident direction Ω' being scattered within an element of solid angle $d\Omega$ with direction Ω . Additional information about phase function: see Liou (2002, ch. 3), Zdunkowski et al. (2007, ch 2).

- $a_{11} = a_{22}$, $a_{21} = a_{12}$. Solutions of Eqs. (A2.1) are described in Ceballos (2021).
- For conservative transfer, $\omega=1$ and $a_{11} = a_{12} = a_{21} = a_{22} = \alpha$.
- In the case of Rayleigh scattering we have $g = 0$, $bm = 1/2$, $\alpha=1$.

About solution of 2-flux RTE for conservative transfer

Consider a homogeneous layer with τ = optical depth, direct beam impinging on the top with zenithal angle Z_o ($\cos Z_o = \mu_o$), over ground with reflectance R_s . We are interested in fluxes across the top and the base of such a layer. Boundary conditions are

$$\zeta_{\downarrow}(0)=0, \quad \zeta_{\uparrow}(\tau)=R_s [\exp(\tau/\mu_o) + \zeta_{\downarrow}(\tau)] .$$

We find for $\zeta_{\uparrow}(0) = R_p$ (layer reflectance):

$$R_p(R_s>0) = \left(1 - (1-R_s) \{ 1 - \alpha \tau + (\alpha \mu_o - b_o) [1 - \exp(-\tau/\mu_o)] \} \right) / [1 + (1-R_s) \alpha \tau], \quad (A2.5)$$

$$R_p(R_s=0) = \{ \alpha \tau - (\alpha \mu_o - b_o) [1 - \exp(-\tau/\mu_o)] \} / [1 + \alpha \tau],$$

For global irradiance G on the surface,

$$G = (1 - R_p) / (1 - R_s), \quad (A2.6)$$

$$G(R_s>0) = \{ 1 + (\alpha \mu_o - b_o) [1 - \exp(-\tau/\mu_o)] \} / [1 + (1-R_s) \alpha \tau],$$

$$G_o = G(R_s=0) = \{ 1 + (\alpha \mu_o - b_o) [1 - \exp(-\tau/\mu_o)] \} / [1 + \alpha \tau].$$

Considering that G is the contribution of original G_o plus multiple reflections (through counter-reflectance R^*) within the layer,

$$G = G_o / (1 - R_s R^*), \quad (A2.7a)$$

$$G/G_o = [1 + \alpha \tau] / [1 + (1-R_s) \alpha \tau] \quad \rightarrow \quad R^* = \alpha \tau / (1 + \alpha \tau). \quad (A2.7b)$$

ANNEX 3. Radiative Code: Daily Cycle of UVNIR irradiance

```
%model GL0.2 for UVNIR

%Program GL02uvnirbis: calculation of daily cycle GLuvnir at two
altitudes
%and presents graphical results

% ----- local data -----
anomesdia= 20230820;
latitude= -30; longitude= -65;
Rso= [0.1 0.1];
zoo= [0.1 3]; %km
% -----

astro= fastrododia(anomesdia);
delta= astro(1); dt= astro(2); D2Do= astro(3);

Souvnir= 757; S= Souvnir* D2Do;
Omega= 2*pi/24;
UTC= [1:.5:24]'; Nt= length(UTC);
G= zeros(Nt+2,2);

for altit= 1:2
    zo= zoo(altit); Rs= Rso(altit);
    po= 1018; Ap= 1.0158; Bp= 0.0927; Cp= 0.0182; %MLW
    p= po/(Ap + Bp*zo + Cp*zo*zo); %zo in km

    Kt= zeros(Nt,1); muo= zeros(Nt,1);
    Rp= Kt; As= Kt;
    for t=1:Nt
        tsolar= UTC(t)+(longitude/15) + dt;
        h= Omega*(12- tsolar);
        mu = cos(delta)*cosd(latitude)*cos(h) + sin(delta)*sind(latitude);
        if mu>0
            Ktbis= fKtuvnirbis(p, mu, Rs);
            Kt(t)= Ktbis(1); Rp(t)= Ktbis(2); As(t)= Ktbis(3);
            muo(t)= mu;
        endif
    endfor % ciclo
    ha= acos(- tan(delta)*tand(latitude));
    UTC12= 12 - longitude/15 - dt;
    UTCrise= UTC12 - ha/Omega; UTCdown= UTC12+ ha/Omega;

    GLuvnir= S*muo.*Kt;
    GLuvnir= [GLuvnir; 0;0]; muo=[muo; 0;0];
    utc= [UTC; UTCrise; UTCdown];
    [utc, i]= sort(utc);
    G(:, altit)= GLuvnir(i);
    muo= muo(i);
    GLo= muo*S;

endfor %altitudes
% -----

figure(1); clf
cyco= plot(utc, GLo, '-sm', 'MarkerSize', 3); hold on
cyc1= plot(utc, G(:,1), '-sc', 'MarkerSize', 3); hold on
cyc2= plot(utc, G(:,2), '-sk', 'MarkerSize', 3); hold on
plot(UTCrise ,0, 'sr'); hold on
plot(UTCdown, 0, 'sr'); hold on
```

```

title(['GLuvnir Daily Cycle - ' num2str(anomesdia)], 'FontSize', 13);
legend([cyco cyc1 cyc2], 'TOA', ['z ' num2str(zoo(1)) ' km'], ...
       ['z ' num2str(zoo(2))]);
xlabel('time UTC (hour)', 'FontSize', 12);
ylabel('irradiance (W m-2)', 'FontSize', 12);
to= 6;
latlon= ['[LAT, LON]= [' num2str([latitude longitude]) ']];
text(to+1, 700, latlon); hold on
text(to+1, 660, ['altitude Z [' num2str(zoo) 'km ]']); hold on
text(to+1, 620, ['surface refl. Rs [' num2str(Rso) ']]'); hold on
axis([to 24 0 750])
grid
% -----

```


Function `Ktuvnirbis` calculates Kt index (interval UVNIR) for input (p , μ_o , R_s)

```
function Ktbis= fKtuvnirbis(p, muo, Rs)
%output [Ktuvnir Rp As] - Rp, As: components of Kto
% -----
psi= p/1000;
z= 14.757 - 22.330*psi + 7.7401 *psi*psi ;    %MLW
% calculo Kto
Aa= 0.342; Ba= 21.7; Ca= -3.28;
As= Aa/(1 + Ba*muo + Ca*muo*muo);

Ar= .353+ .099*psi;
beta= 5.369; alfa= -0.860; Br= beta*psi^alfa;
Cr= 1.309*psi^3 - 3.530* psi^2 + 3.216*psi - 0.915;
Rp= Ar/(1+ Br*muo + Cr*muo*muo);

Kto= 1 - Rp - As;
% -----
% calculo Kt

Bmed= -.334; Cmed= .171; Az= 0.102 - 0.008*z;    %z em km
Ra= Az/(1+ Bmed*muo + Cmed*muo*muo);

Ktuvnir= Kto/(1 - Rs * Ra);
Ktbis= [Ktuvnir Rp As];
% -----
endfunction
```

Function `astrododia` evaluates declination δ , sun-earth relative distance $(D/D_o)^2$ and time equation δt for input `anomesdia`.

```
function astro= fastrododia(anomesdia)
%versao corrigida abril 2017
% calcula declinacao (radianos)e equacao do tempo (horas)
%a partir da data anomesdia [yyyymmdd]
dia0= [0 31 59 90 120 151 181 212 243 273 304 334];
diasdoano= 365;
ano= floor(anomesdia/10000); mesdia= mod(anomesdia,10000);
mes= floor(mesdia/100); dia= mod(mesdia,100);
if mod(ano,4)==0
    dia0= dia0 + [0 0 1 1 1 1 1 1 1 1 1 1];
    diasdoano= diasdoano+1;
end
diajul= dia0(mes)+ dia;
teta = 2 * pi * (diajul-1) / diasdoano; %radianos
delta = .006918 - .399912 * cos(teta) + .070257 * sin(teta) - ...
        .006758 * cos(2 * teta) + .000907 * sin(2 * teta) - ...
        .002697 * cos(3 * teta) + .00148 * sin(3 * teta); %radianos
dtempo= .000075 + .001868* cos(teta) - .032077* sin(teta) - ...
        .014615 * cos(2 * teta) - .040849* sin(2*teta); %radianos
dt= dtempo*180/(pi*15); %horas

r2sun = 1.00011 + .034221 * cos(teta) + .000128 * sin(teta) +...
        0.000719* cos(2*teta) + 0.000077* sin(2*teta);
%algoritmo corrigido - Paltridge & Platt 1976
%r2sun= (Do/D)^2
astro= [delta; dt; r2sun];
endfunction
```

